**Direct epicardial assist device using artificial rubber muscle in a swine model of pediatric dilated cardiomyopathy.**

(人工ゴム筋肉を用いた心補助装置の開発とブタ小児拡張型心筋症モデルにおける血行動態的評価)

申請者　　弘前大学大学院医学研究科
機能再建再生科学領域 再生再建理論外科学教育研究分野

氏名　　齊藤　良明
指導教授　　福田　幾夫

Abstract

Purpose: Ventricular assist devices are a potent alternative or bridge therapy to heart transplants for dilated cardiomyopathy patients. However, ventricular assist devices have problems related to biocompatibility, hemocompatibility, and thromboembolic events, especially in younger patients. The present study examined the hemodynamic effects of a direct cardiac compression device using circumferential artificial rubber muscles in a young swine model of dilated cardiomyopathy.

Methods: Dilated cardiomyopathy was established in 6 pigs (6-8 weeks of rapid right ventricular pacing; average weight, 22.6 ± 2.1 kg). The device was designed using pneumatic rubber muscles (Fluidic Muscle, Festo). Hemodynamic parameters were monitored under baseline conditions, after the assistance, and after inducing ventricular fibrillation. Hemodynamic data were acquired using a PiCCO, multilumened thermodilution catheter in the pulmonary artery, left ventricular pressure monitoring, and epicardial echocardiography.

Results: Direct epicardial assistance resulted in a significant improvement in hemodynamic data. Cardiac output improved from 1.39 ± 0.24 L/min to 1.96 ± 0.46 ($p = 0.02$). Stroke volume (14.5 ± 3.2 mL versus 20.1 ± 4.3 ml, $p<0.01$) and ejection fraction (25.2 ± 3.6% versus 47.7 ± 7.8%, $p<0.01$) also improved after assistance. After inducing ventricular fibrillation, cardiac output was maintained at 1.33 ± 0.28 L/min.

Conclusions: Use of a circumferential direct epicardial assistant device resulted in improvement in hemodynamic data in a dilated cardiomyopathy model. Although there is still a need for improvements in device components, the direct cardiac assist device may be a good alternative to recent heart failure device therapies.

Keywords: Blood vessel prosthesis, Artificial muscle, Cardiac support

## 1. Introduction

Dilated cardiomyopathy (DCM) is a heart muscle disorder defined by the presence of a dilated and poorly functioning left ventricle in the absence of systemic hypertension, valve disease, and ischemic heart disease (1). DCM accounts for 30% to 40% of all heart failure cases in large clinical trials and is the leading cause of heart transplantation (2, 3).

Ventricular assist devices (VAD) are used as a bridge therapy to heart transplant or as a permanent solution for heart failure. Ongoing refinements in technology have led to improved patient outcomes and device durability, although problems related to biocompatibility, hemocompatibility, infection and thromboembolic or hemorrhagic events remain (4-7).

DCM is the most common pediatric cardiomyopathy, an important cause of heart failure and a leading cause of heart transplantation in children (8-11). Despite recent medical advances, event-free survival remains poor, with 5-year rates of death or transplantation reported as high as 46% (9). Similar to adult patients, VAD can be applied to pediatric patients, although there have been smaller device options available. The Berlin Heart EXCOR is one option, although it is still associated with thromboembolic and hemorrhagic events with high mortality (12-14). Therefore, other options are needed.

Recently, artificial rubber muscle has been utilized in various robotic devices for rehabilitation in people with walking difficulties as well as in nursing care that involves heavy laborious work (15-17). In the present study, we evaluated the effect of a novel direct epicardial compressive device using artificial muscles on hemodynamics in young swine DCM models.

## 2. Material and methods

The immediate effects of a non-blood-contacting epicardial assist device were studied in a porcine DCM model. The device consisted of two circumferential rubber muscles (Fluidic Muscle, FESTO, Esslingen, Germany) of which ends were fixed at a 50 mm stainless steel bar through 30 mm-long reinforced polyethylene connectors (Fig 1AB). Device body weight

including rubber muscles, connectors and the stainless steel bar was 50 g. Characteristics of the rubber muscles have been documented previously. [18,19] Briefly, the muscle is formed by a pressure-tight rubber hose and is 5 mm in diameter. The driving force is compressed air. Maximal permissible contraction is 25% of the normal length. The device was composed of actuators, pressure sensors (PSE510-M5, SMC Co., Tokyo, Japan), solenoid valves (BV214A-CB0-00-BCNA-CTA, MAC Valves, Inc., Dundee, MI), micro-sequencers (FX1N-40MT, FX2N-16EXL-C, Mitsubishi Electric Corporation, Tokyo, Japan) and an air compressor.

With approval from the Institute of Animal Experiments of the Hirosaki University Graduate School of Medicine, six male crossbred pigs were used in this study. All pigs were treated and cared for in accordance with the Fundamental Guidelines for Proper Conduct of Animal Experiment and Related Activities in Academic Research Institutions under the jurisdiction of the Japanese Ministry of Education, Culture, Sports, Science and Technology. [20] Six pigs (average weight, 10.8 ± 0.8 kg) underwent pacemaker implantation, followed by delayed loading of a new direct epicardial assist device. Additionally, six healthy weight-matched controls (average weight, 22.3 ± 2.3 kg) were used for hemodynamic comparisons.

DCM induction

Treatment pigs were sedated with intramuscular injection of 30 mg/kg ketamine, followed by intravenous bolus injection of 0.1 mg/kg midazolam. After intubation with mechanical ventilation, general anesthesia was maintained by intravenous continuous infusion of midazolam (0.1-0.2 mg/kg/hr) and remifentanil hydrochloride (0.25 μg/kg/min). A bipolar tined pacing lead (CapSure Z Novus 5054, Medtronic, Minneapolis, MN) was inserted into the left internal jugular vein and positioned in the right ventricular apex. The lead was connected to a pacemaker (Adapta DR, Medtronic), and the pacing system was placed in a subcutaneous pocket. The pacemaker was activated for right ventricular pacing at 170 beats per minute. A 1:1 rate of capture was verified via electrocardiographic recordings and echocardiography. Electrocardiographic recordings were performed

frequently during the pacing protocol to ensure continuous capture. After 6 to 8 weeks of active pacing, the pigs were returned to the laboratory for deactivating pacing and device implantation.

Hemodynamic data measurements

The average weight of DCM models at terminal study was 22.6 ± 2.1 kg. Tracheostomy was performed, and a tracheal tube was placed. Anesthesia was maintained with intravenous continuous infusion of midazolam (0.1-0.2 mg/kg/hr) and remifentanil hydrochloride (0.25 μg/kg/min). A bolus of vecuronium (0.04 mg/kg) was administered every 20 minutes during the procedure. Intravenous infusion of amiodarone was initiated at 0.5 mg/kg/hr. After stabilization of the anesthesia, a multi-lumened thermodilution catheter was positioned in the pulmonary artery via the right external jugular vein for the measurement of pulmonary capillary wedge pressure (PCWP), pulmonary artery pressure (PAP), and central venous pressure (CVP). The left femoral artery was cut down and a PiCCO pressure catheter (PULSION Medical Systems SE, Feldkirchen, Germany) was placed intraaortically for hemodynamic measurements. The catheter was connected to its monitoring device (PiCCO2 PC8500US, PULSION Medical Systems SE). After the median sternotomy and pericardiotomy were performed, a 4-Fr catheter sheath (Avanti Catheter Sheath Introducers 504-604P, Cordis Corporation, Miami Lakes, FL, USA) was inserted from the apex of the heart directly, was connected to a dual pressure monitor (BSM9510, Nihon Kohden Co., Tokyo, Japan), and was captured at 1000 Hz using a Keyence multi-data acquisition system (NR-500, Keyence Co.) with an analog to digital converter (NR-HA08, Keyence Co.). Recorded left ventricular pressure (LVP) data were analyzed using NR-H7W software (WAVE LOGGER, Keyence Co.). Direct epicardiac echo was performed to obtain visual data and left ventricular ejection fraction (LVEF). Mitral regurgitant fraction was calculated by antegrade and retrograde flow analysis at the aortic annulus and mitral annulus.

Device characteristics and implantation

A bipolar temporary myocardial pacing lead (Streamline, Medtronic, Minneapolis, MN) was placed in right atrium to capture autonomic p wave and was connected to a pacemaker programmer (Medtronic CareLink® 2090, Medtronic). A 90 bpm DDD pacing mode (atrioventricular (AV)-delay of 200 msec) with output voltage of 5V was initiated. A 5V power voltage was input to the micro-sequencer, and the sequence program was driven. The micro-sequencer control of the solenoid valve opening was done through the ladder logic program. The duration of muscle contraction/dilatation and driving pressure was preset to 200/300 msec and 0.6 MPa, respectively. The schematic device system is summarized in Fig. 2A.

The circumferential length of hearts at 1 cm below the atrioventricular groove and the mid-portion between the atrioventricular groove and apex was respectively measured, and an appropriate length (50 to 55 mm shorter than measured length) of the artificial muscle was tailored. Two muscles were fixed at a stainless bar at both ends through 30 mm long plastic connectors. Then, a saccular-shape muscle device was loaded from the apex of the heart to just below the atrioventricular groove. (Fig. 2B) The device itself was fixed at both sides of the clavicle bones using umbilical tape.

Experimental protocol and data analysis

Steady state hemodynamics, specifically heart rate, atrial blood pressure, CVP, PAP, PCWP, LVP, and echocardiographic LVEF with end-diastolic volume and end-systolic volume were recorded with the ventilator temporarily suspended to prevent respiratory artifact. Cardiac output using pulse contour analysis by the PiCCO system was also obtained. Other circulatory parameters, including stroke volume (SV), systemic vascular resistance (SVR), maximum dP/dt, global ejection fraction (GEF), and cardiac power output (CPO), were also obtained. Measured data points were before loading the device, after the assistance with the device, and after inducing ventricular fibrillation by injecting 15% potassium chloride (20 ml) intravenously while assisting. After obtaining all hemodynamic data, the device was turned off, and each study was terminated.

All numerical circulatory data are presented as means ± standard deviations and were assessed using a paired Student's t test. Statistical analyses were performed using the SPSS statistical software version 20 (IBM, Armonk, NY), and at p value less than 0.05 was used as an indicator of statistical significance.

## 3. Results

All hemodynamic data indicated the successful establishment of DCM pig models by rapid right ventricular pacing. In echocardiographic data, decreased LVEF (25.2 % ± 3.6% vs. 59.0% ± 6.8%), and increased EDV (44.0 ± 12.2 ml vs. 32.7 ± 9.2 ml) were observed when compared with healthy weight-matched controls. PAP and PCWP were relatively high in the DCM model (14.2 ± 3.5 mmHg vs. 12.8 ± 2.9 mmHg), with lower left ventricular pressure (105.1 ± 23.5 mmHg vs. 139.1 ± 4.6 mmHg), reflecting left ventricular dysfunction. CO and SV was markedly decreased in DCM models (1.39 ± 0.24 L/min vs. 3.14 ± 0.46 L/min, 14.5 ± 3.3 ml vs. 30.8 ± 7.6 ml) when compared with controls.

Device feasibility in synchronization

The device worked regularly, coordinating with native heart movement, and result in improvements in hemodynamics. Series of ventricular arrhythmias were not observed during assistance. Ventricular function significantly improved when receiving synchronous epicardiac assistance, with EF increasing from 25.2% ± 3.6% to 47.7% ± 7.8% ($p < 0.01$) and CO increasing from 1.39 ± 0.24 L/min to 1.96 ± 0.46 L/min (ΔCO ranged from 0.29 L/min to 0.9 L/min). EDV appropriately remodeled from 44.0 ± 12.2 ml to 35.0 ± 12.1 ml while SV increased from 14.5 ± 3.3 ml to 20.1 ± 4.3 ml. Left ventricular pressure did not significantly change, while SVR markedly decreased from 4786 ± 1022 dynes・sec・$cm^{-5}$ to 3960 ± 844 dynes・sec・$cm^{-5}$ ($p = 0.09$), which corresponded with an improvement in output. Heart rate did not significantly change after the assistance (96.8 ± 7.3 bpm before the assistance, 97.1 ± 6.7 bpm after the assistance). Hemodynamic variables are

summarized in Table 1. Configuration of left ventricular pressure demonstrated early notch in the systolic phase, indicating contraction support by the epicardiac assist device (Fig. 3A,B).

The steady state of DCM models in both the unassisted and assisted condition demonstrated evidence of mitral regurgitation. However, no difference was observed in the mitral regurgitant fraction between the two conditions (13.6% ± 4.2% vs. 15.2% ± 5.1%, p = 0.58)

Table 1. Summary of Hemodynamic Variables

| Variables | Controls | Unassisted | Assisted | Ventricular fibrillation |
|---|---|---|---|---|
| Cardiac output, L/min | 3.14 ± 0.46 | 1.39 ± 0.24[a] | 1.96 ± 0.47[b] | 1.33 ± 0.28 |
| Ejection fraction, % | 59.0 ± 6.8 | 25.2 ± 3.6[a] | 47.7 ± 7.8[b] | 28.1 ± 3.2 |
| Stroke volume, ml | 30.8 ± 7.6 | 14.5 ± 3.3[a] | 20.1 ± 4.3[b] | 13.0 ± 4.9 |
| Left ventricular end-diastolic volume, ml | 32.7 ± 9.2 | 44.0 ± 12.2 | 35.0 ± 12.1 | 25.3 ± 9.4 |
| Systemic vascular resistance, dynes•sec•$cm^{-5}$ | 2692 ± 1188 | 4786 ± 1022[a] | 3960 ± 844 | 2526 ± 1566 |
| Maximum dP/dT, mmHg/sec | 698.1 ± 104.6 | 375.0 ± 78.7[a] | 388.6 ± 68.9 | 297.1 ± 76.5 |
| Cardiac power output, $w/m^2$ | 0.70 ± 0.12 | 0.26 ± 0.08 | 0.40 ± 0.16[b] | 0.15 ± 0.08 |

| | | | | |
|---|---|---|---|---|
| Heart rate, beat/min | 99.8 ± 6.3 | 96.8 ± 7.3 | 97.1 ± 6.7 | 102.0 ± 14.4 |
| Peak systemic blood pressure, mmHg | 138.6 ± 21.2 | 118.8 ± 17.9 | 124.3 ± 20.2 | 74.5 ± 21.7 |
| Peak left ventricular pressure, mmHg | 139.1 ± 4.6 | 105.1 ±23.5[a] | 107.3 ± 24.5 | 73.1 ± 22.1 |
| Central venous pressure, mmHg | 12.3 ± 1.3 | 13.0 ± 3.2 | 15.0 ± 3.8 | 21.5 ± 3.4 |
| Peak pulmonary arterial pressure, mmHg | 31.3 ± 4.5 | 34.5 ± 5.0 | 34.5 ± 3.8 | 40.4 ± 9.7 |
| Pulmonary capillary wedge pressure, mmHg | 12.8 ± 2.9 | 14.1 ± 3.4 | 15.6 ± 3.5 | 22.6 ± 7.2 |

"a" denotes $p < 0.05$ when comparing healthy controls with DCM models by two sample t test.

"b" denotes $p < 0.05$ when comparing unassisted state with assisted state by paired t test.

Mandatory epicardiac support in ventricular fibrillation

After inducing ventricular fibrillation, mandatory device activation was initiated (Fig. 4A,B). Heart rate was set ranging from 90 bpm to 120 bpm by modulating pacemaker programmer. After steady state was obtained, each parameter was measured. CO could still be measured with an average value of 1.33 ± 0.28 L/min. SV was 13.0 ± 4.9 ml, and maximum dP/dT was 297 ± 76 mmHg/sec. Average peak systolic left ventricular pressure (depicted in Fig. 3C) and LVEF was 73.1 ± 22.1 mmHg and 28.1% ± 3.2%, respectively. Systolic and diastolic PAP, PCWP, and CVP were all elevated with an average value of 40.4 ± 9.7 mmHg, 26.4 ± 9.3 mmHg, 22.6 ± 7.2 mmHg, and 21.5 ± 3.4 mmHg, respectively. These data indicated biventricular insufficiency, although dilation of pupils and gasping respiration were not

evident during the support. Ventricular perforation or bleeding was not observed.

## 4. Discussion

This study demonstrated the efficacy of a circumferential epicardial assist device in DCM pig models. Six young pigs underwent DCM induction by a relatively low right ventricular pacing rate of 170 bpm for 6 to 8 weeks, which resulted in the development of increased EDV size and low EF and CO, indicating successful establishment of DCM models. Previous studies showed the development of tachycardia-induced heart failure in response to 220 to 240 bpm for 1 to 3 weeks in pigs weighing 25 to 45 kg [21-24]. We implanted pacemakers in 6 pigs (weight, 10-12 kg) in order to get smaller DCM models that approximate young children. Lionetti et al induced heart failure in mature mini-pigs by a relatively low pacing rate of 180 bpm, [25] and Paslawska et al induced a cardiomyopathy model by chronic pacing of 170 bpm for 4 to 28 weeks in adult pigs weighing 70 to 74 kg [26]. These studies demonstrated a 47% to 67% decrease in EF when compared with controls, which corresponds to the data from our DCM model.

The positive hemodynamic effects of this device were represented by increasing CO, SV and LVEF with moderate approximation of EDV. EF increased from 25.2% ± 3.6% to 47.7% ± 7.8% after the assistance. It is true that this result should be carefully interpreted, because this was not a double-blind study and could be subject to bias. With regard to objective data, CO increased from 1.39 ± 0.24 L/min to 1.96 ± 0.46 L/ min after the assistance, and its increment ranged from 0.29 to 0.9 L/min. This increment represents a wide range and may not be truly satisfactory, because CO after assistance did not reach the level of that in control pigs (3.14 ± 0.46 L/min).

This prototype device currently has some problems in its design. For example, it is difficult to determine the appropriate length of artificial muscle in each heart. If the muscle length is too long, hemodynamic assistance will become less effective. If the muscle length is too short, it might cause diastolic dysfunction and ventricular arrhythmias, resulting in

further deterioration of the hemodynamic state. It is essential to determine the appropriate length of muscles in order to obtain maximum hemodynamic support. We need to invent a new device design that enables us to adjust muscle length flexibly and easily. As for device fitting, mesh fixation is likely to be effective, so as not to slip out from the ventricles. Positioning might also be a key to successful assistance, because too high positioning near the atrioventricular groove may cause mitral regurgitation, resulting in inefficient blood flow towards the left ventricular outflow tract. The pneumatic muscle itself needs to gain more flexibility and elasticity so as to fit the heart surface in a gentle fashion.

Computational fluid dynamics are valuable methods of visualizing left ventricular geometry and material property. [27-30] These tools will be essential for optimization of the device and ventricular functioning going forward. Cardiac magnetic resonance imaging is a novel approach for visualizing dynamic flow, [30, 31] which can be utilized to analyze the therapeutic efficacy of this device, as it is technically possible to make the device completely non-ferromagnetic.

In synchronizing the native heart, the mechanism of supporting the heart by this device is composed of two different factors: extrinsic pumping action of the device contributing to the systolic ejection, and augmentation of autonomic contraction by accelerating wall movement. Contracting the device in the end-systolic phase (as in accelerating pendulum swings) leads to an increase in effective ventricular output. Therefore, it is essential to precisely control the contraction timing of the device. This was a preliminary study, and we fixed primarily the AV-delay and contractile duration at 200 msec. AV delay can be modulated by pacemaker programming, and contractile duration can be modulated by the ladder logic program of the micro-sequencer. Investigators previously studied an in vitro study of this artificial muscle device. [19] In that study, the muscle could contract in 100 msec or longer. Analysis of contraction timing on each cardiac cycles will be performed in future studies.

When ventricular fibrillation was induced, autonomic contractility was lost, and the device worked mandatorily. Systemic CO was maintained at 1.33 ±

0.28 L/min, LVP was maintained at 73.1 ± 22.1 / 14.7 ± 3.7 mmHg, and systemic pressure was maintained at 74.5 ± 21.7 / 58.0 ± 21.5 mmHg. There was no sign of brainstem death, and systemic organ function was likely to be maintained. Global biventricular support was achieved without atrial movements. However, elevation of PAP and PCWP were observed; thus, it is likely to be difficult to maintain whole body circulation in the chronic phase. The artificial muscle has a property of 25% contraction of nominal length in the longitudinal direction, according to the manufacturer. This means an ejection fraction of approximately 44% can theoretically be maintained if the device would form a fully covered jacket model by increasing the number of artificial muscles and by filling the interspaces of the present prototype model.

There are other ventricular support devices for direct epicardiac assistance. The CorCap Cardiac Support Device (Acorn Cardiovascular, Inc., St. Paul, MN) [32-34], and the HeartNet Implant (Paracor Medical, Inc., Sunnyvale, CA) have advanced to clinical trials. [35,36] Both studies demonstrated improvements in end-diastolic and end-systolic volumes of the heart. These two devices are passive support devices that provide a restraint effect via sustained transmural myocardial pressure. McGarvey et al. reported a novel device for active epicardiac ventricular support in ischemic cardiomyopathy. [30] This device utilizes a rubber inflatable bladder that is positioned and fixed at the dyskinetic infarcted area. Use of this device resulted in improvement in hemodynamics, including EF, which increased from 26.0% ± 4.8% to 37.3% ± 4.5% after the assistance. Its concept is similar to our device, although that device is specialized for ischemic cardiomyopathy and represents focal support rather than global support and therefore might not be applicable to the global ventricular impairment of DCM. DCM is commonly accompanied by right ventricular dysfunction. [37] The pathophysiology of heart failure is likely to be different in children than in adults. [12] Isolated left ventricular dysfunction is rare in children, in whom the need for circulatory support is often due to a combination of right ventricular failure, hypoxemia and pulmonary hypertension. The full jacket device presented in this report might be able to support both the left and the

right ventricles, because the artificial muscles contract in a concentric fashion, and therefore, its force of contractility may conduct equally to both ventricles. This topic should be assessed in future studies. To advance this device to clinical use, frictional force against the epicardiac surface and heat production by prolonged continuous driving may have to be resolved. Too much frictional force may result in ventricular perforation and bleeding, and the heat may cause protein degeneration leading to further ventricular deterioration. There was no perforation or bleeding observed in this acute preliminary study. Chronic device placement will be the focus of future studies.

In conclusion, a circumferential direct epicardiac assist device resulted in improvement in hemodynamic data in a young DCM model in this preliminary study. Although further work is needed to analyze its characteristics and there is still a need for improvements in device components, this direct cardiac assistance device may be a good alternative to recent heart failure device therapies for this subset of pathology.

Acknowledgements
We thank Akio Toyoda and Tooru Norita for their technical support.

Disclosures
Financial support: This work was supported by JSPS KAKENHI Grant Number 24659581.
Conflict of interest: None declared.
Meeting presentations: Presented in part at the 42nd Congress of the European Society for Artificial Organs, held September 2 to 5, 2015 in Leuven, Belgium.

References

[1] Elliott P. Diagnosis and management of dilated cardiomyopathy. Heart 2000;84:106-112.

[2] McNally EM, Golbus JR, Puckelwartz MJ. Genetic mutations and mechanisms in dilated cardiomyopathy. J Clin Invest 2013;123:19–26.

[3] Haas J, Frese KS, Peil B, et al. Atlas of the clinical genetics of human dilated cardiomyopathy. Eur Heart J. 2015;36:1123-1135.

[4] Pozzi M, Giraud R, Tozzi P, et al. Long-term continuous-flow left ventricular assist devices (LVAD) as bridge to heart transplantation. J Thorac Dis 2015;7:532-542.

[5] Miller LW, Pagani FD, Russell SD, et al. Use of a continuous-flow device in patients awaiting heart transplantation. N Engl J Med 2007;357:885-896.

[6] John R, Kamdar F, Liao K, Colvin-Adams M, Boyle A, Joyce L. Improved survival and decreasing incidence of adverse events with the HeartMate II left ventricular assist device as bridge-to-transplant therapy. Ann Thorac Surg 2008;86:1227-1234.

[7] Lok SI, Martina JR, Hesselink T, et al. Single-centre experience of 85 patients with a continuous-flow left ventricular assist device: clinical practice and outcome after extended support. Eur J Cardiothorac Surg 2013;44:e233-238.

[8] Daubeney PE, Nugent AW, Chondros P, et al. Clinical features and outcomes of childhood dilated cardiomyopathy: results from a national population-based study. Circulation 2006; 114:2671–2678.
[9] Towbin JA, Lowe AM, Colan SD, et al. Incidence, causes, and outcomes of dilated cardiomyopathy in children. JAMA. 2006;296:1867–1876.

[10] Molina KM, Shrader P, Colan SD, et al. Predictors of disease progression in pediatric dilated cardiomyopathy. Circulation: Heart Failure 2013;6:1214-1222.

[11]den Boer SL, Lennie van Osch-Gevers M, van Ingen G, et al. Management of children with dilated cardiomyopathy in The Netherlands: Implications of a low early transplantation rate. J Heart Lung Transplant. Epub 2015 Feb 7.

[12] Gournay V, Hauet Q. Mechanical circulatory support for infants and small children. Arch Cardiovasc Dis 2014;107:398-405.

[13] Almond CS, Morales DL, Blackstone EH, et al. Berlin heart EXCORE pediatric ventricular assist device for bridge to heart transplantation in US children. Circulation 2013;127:1702-1711.

[14] Cassidy J, Dominguez T, Haynes S, et al. A longer waiting game: bridging children to heart transplant with the Berlin Heart EXCOR device--the United Kingdom experience. J Heart Lung Transplant 2013;32:1101-1106

[15] Morales R, Badesa FJ, Garcia-Aracil N, Sabater JM, Perez-Vidal C. Pneumatic robotic systems for upper limb rehabilitation. Med Biol Eng Comput. 2011;49:1145-1156

[16] Zhang H, Balasubramanian S, Wei R, et al. RUPERT closed loop control design. Conf Proc IEEE Eng Med Biol Soc. 2010;10:3686-3689

[17] Kobayashi H, Nozaki H, Tsuji T. Development of power assist system for caregiver by muscle suit. Proceeding of the 2007 IEEE International Conference on Mechatronics and Automation. 2007; Aug 5-8, Harbin, China. p.180-5. Available from: http://ieeexplore.ieee.org/stamp/stamp.jsp?tp=&arnumber=4303537

[18] FESTO AG & Co. KG [Internet]. Innovation and technology: Fluidic muscle [cited 2013 Jun 24]. Available from:

http://www.festo.com/cms/en_corp/9790.htm
[19] Saito Y, Suzuki Y, Goto T, Daitoku K, Minakawa M, Fukuda I. Cardiac supporting device using artificial rubber muscle: preliminary study to active dynamic cardiomyoplasty. J Artif Organs 2015, Epub ahead of print

[20] Fundamental Guidelines for Proper Conduct of Animal Experiment and Related Activities in Academic Research Institutions under the jurisdiction of the Ministry of Education, Culture, Sports, Science and Technology (Ministry of Education, Culture, Sports, Science and Technology, Notice No. 71) [Internet] [updated and sited 2006 Jun 1] available at http://www.lifescience.mext.go.jp/policies/pdf/an_material011.pdf

[21] Spinale FG, Zellner JL, Tomita M, Crawford FA, Zile MR. Relation between ventricular and myocyte remodeling with the development and regression of supraventricular tachycardia-induced cardiomyopathy. Circ Res 1991;69:1058-1067.

[22] Hendrick DA, Smith AC, Kratz JM, Crawford FA, Spinale FG. The pig as a model of tachycardia and dilated cardiomyopathy. Lab Anim Sci 1990;40:495-501.

[23] Bauer A, McDonald AD, Donahue JK. Pathophysiological findings in a model of persistent arterial fibrillation and severe congestive heart failure. Cardiovasc Res 2004;61:764-70.

[24] Dixon JA, Goodman AM, Gaillard II WF, et al. Hemodynamics and myocardial blood flow patterns after placement of a cardiac passive restraint device in a model of dilated cardiomyopathy. J Thorac Cardiovasc Surg 2011;142:1038-1045.

[25] Lionetti V, Guiducci L, Simioniuc A, et al. Mismatch between uniform increase in cardiac glucose uptake and regional contractile dysfunction in pacing-induced heart failure. Am J Physiol 2007;293:H2747-2756.

[26] Palawska U, Gajec J, Kiczak L, et al. Development of porcine model of chronic tachycardia-induced cardiomyopathy. Int J Cardiol 2011;153:36-41.

[27] Khalafvand SS, Ng EY, Zhong L. CFD simulation of flow through heart: a perspective review. Comput Methods Biomech Biomed Engin. 2011; 14:113-132.

[28] Nguyen VT, Loon CJ, Nguyen HH, Liang Z, Leo HL. A semi-automated method for patient-specific computational flow modelling of left ventricles. Comput Methods Biomech Biomed Engin 2015;18:401-413.

[29] Fraser KH, Taskin ME, Griffith BP, Wu ZJ. The use of computational fluid dynamics in the development of ventricular assist devices. Med Eng Phys 2011;33:263-280.

[30] McGarvey JR, Kondo N, Takebe M, Koomalsingh KJ, Witschey WRT, Barker AJ, et al. Directed epicardial assistance in ischemic cardiomyopathy: flow and function using cardiac magnetic resonance imaging. Ann Thorac Surg 2013;96:577-585.

[31] Moosavi MH, Fatouraee N, Katoozian H, Pashaei A, Camara O, Frangi AF. Numerical simulation of blood flow in the left ventricle and aortic sinus using magnetic resonance imaging and computational fluid dynamics. Comput Methods Biomech Biomed Engin 2014;17:740-749.

[32] Power JM, Ramen J, Dornom A, et al. Passive ventricular constraint amends the course of heart failure: a study in an ovine model of dilatated cardiomyopathy. Cardiovasc Res 1999;44:549-555.

[33] Saavedra WF, Tunin RS, Paolocci N, et al. Reverse remodeling and enhanced adrenagic reserve from a passive external ventricular support in experimental dilated heart failure. J Am Coll Cardiol 2002;39:2069-2076.

[34] Mann DL, Acker MA, Jessup M, Sabbah HN, Starling RC, Kubo SH. Clinical evaluation of the CorCap Cardiac Support Device in patients with dilated cardiomyopathy. Ann Thorac Surg 2007;84:1226-1235.

[35] Magovern JA. Experimental and clinical studies with the Paracor cardiac restraint device. Semin Thorac Cardiovasc Surg. 2005;17:364-368.

[36] Klodell CT, Aranda JM, McGiffin DC, et al. Worldwide surgical experience with the Paracor HeartNet cardiac restraint device. J Thorac Cardiovasc Surg. 2008;135:188-195

[37] Oyama S, Sakuma M, Komaki K, et al. Right ventricular systolic function and the manner of transformation of the right ventricle in patients with dilated cardiomyopathy. Circ J. 2004;68:933-937.

## Figure Legends

Fig. 1 - (A) Device appearance in the diastolic phase. Two rubber artificial muscles are used. Muscle lengths are determined by measuring the circumferential length of hearts at 1 cm below the atrioventricular groove and at the midportion between atrioventricular groove and apex. Muscles are trimmed 50 to 55 mm shorter than these lengths, because the plastic connectors on both ends are 30 mm long. Both ends of muscles are fixed at the stainless bar, forming a circular shape. (B) Systolic phase. The device contracts in a concentric fashion.

Fig. 2 - (A) Schema of the device control system. Atrial p wave is captured by a pacemaker programmer that works as a DDD pacemaker with a lower rate of 90 beat/min. A 5-V output from the programmer triggers the micro-sequencer that sends control signals to on/off solenoid valves. The sequencer is controlled by a ladder logic program that is installed from a computer. Compressed air is supplied by the air compressor. A pressure

sensor monitors the supplied air pressure inside the driveline and provides a feedback signal to the sequencer. (B) Intraoperative finding of the heart after loading and driving the device during ventricular fibrillation.

Fig. 3 - Configuration of left ventricular pressure pulse wave. (A) Unassisted. (B) Assisted. The device movement might contribute to an early systolic shooting pulse wave. (C) Mandatory support during ventricular fibrillation

Fig. 4 - Echocardiographic findings of the device assistance during ventricular fibrillation. Four-chamber views. (A) Diastolic phase. Cross-section of artificial muscles is observed in the lateral walls of the left and right ventricles. Pacemaker lead for dilated cardiomyopathy induction is positioned in the right ventricle. Mitral valve opens during the diastolic phase without left atrial movement. (B) Systolic phase. Artificial muscles contract and compress the right and left ventricles. Mitral valve is closed.

Fig.1

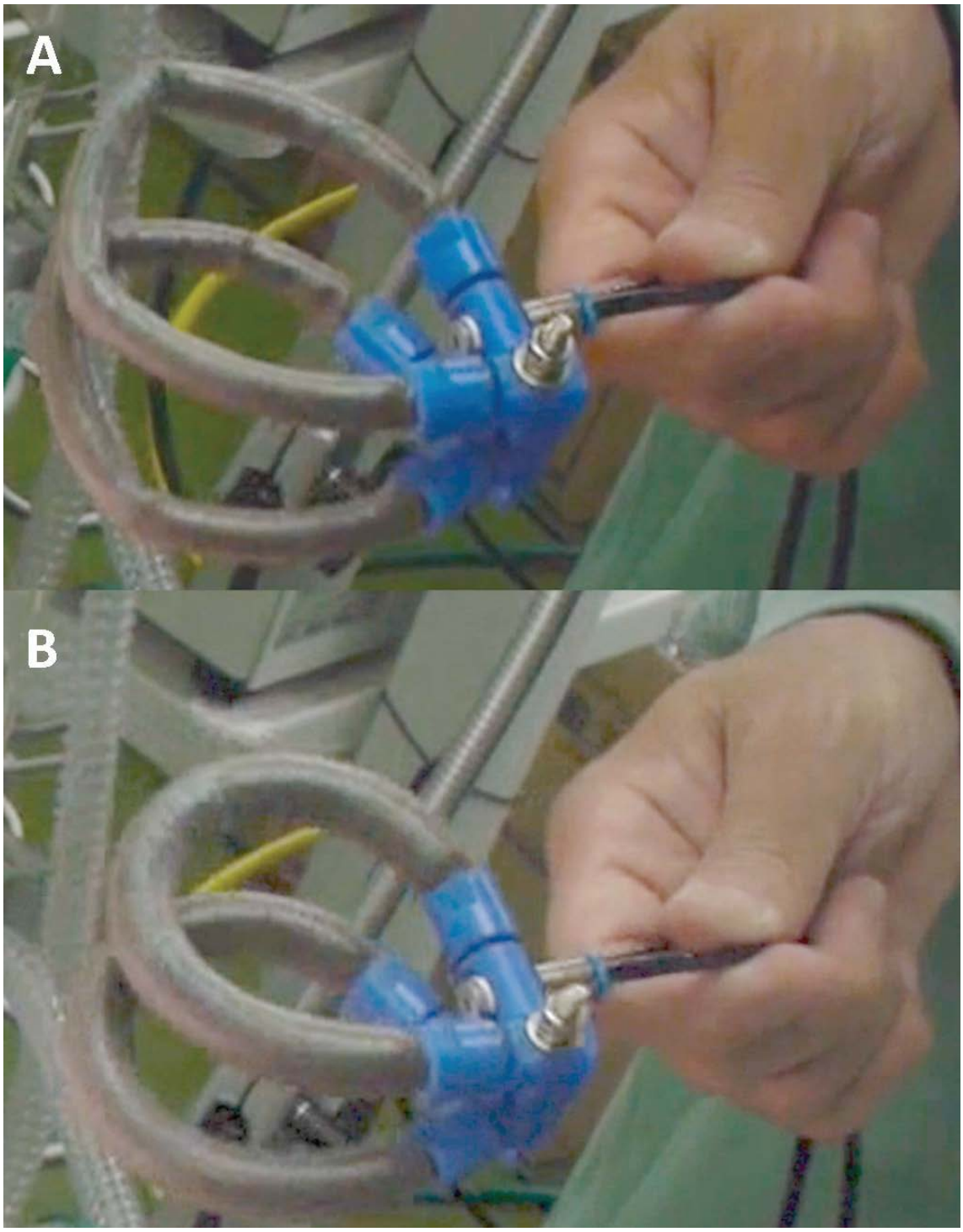

Fig. 2

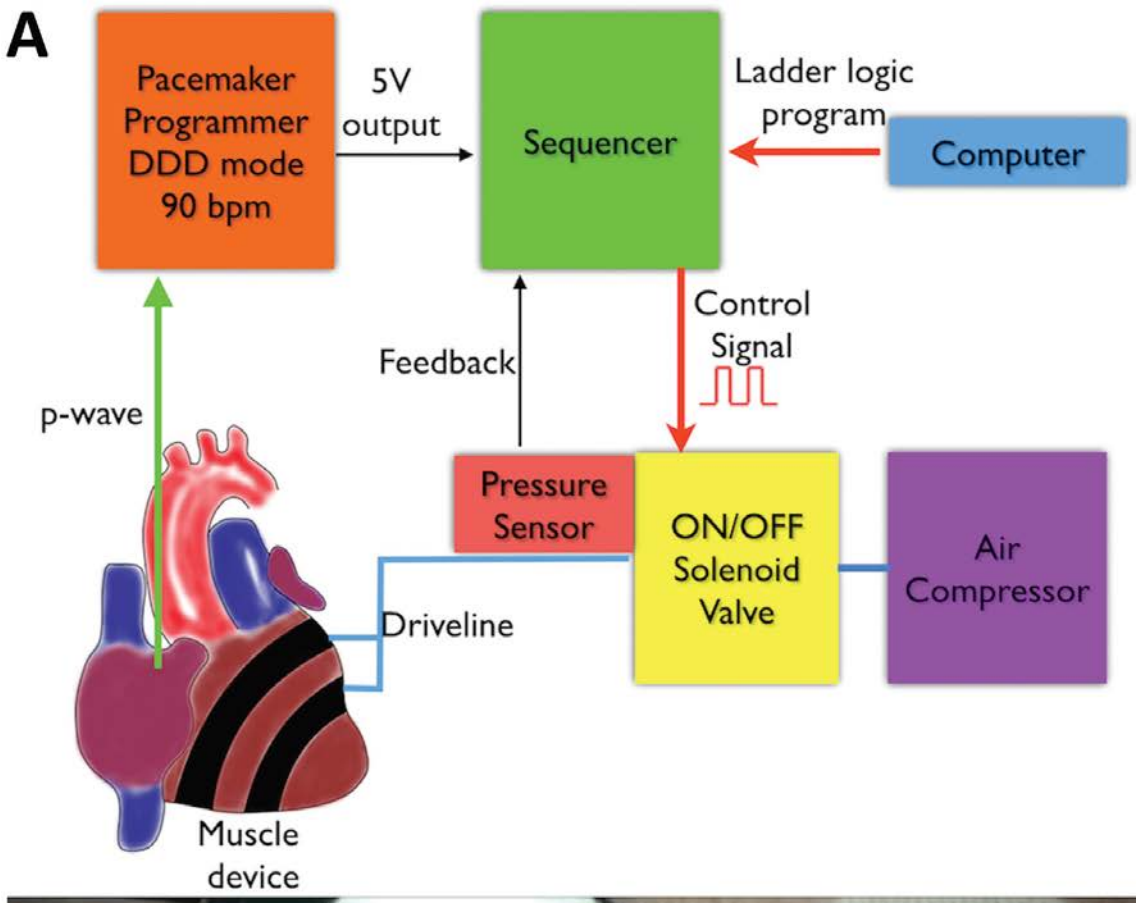
A
Pacemaker Programmer DDD mode 90 bpm
5V output
Sequencer
Ladder logic program
Computer
Control Signal
Feedback
p-wave
Pressure Sensor
ON/OFF Solenoid Valve
Air Compressor
Driveline
Muscle device

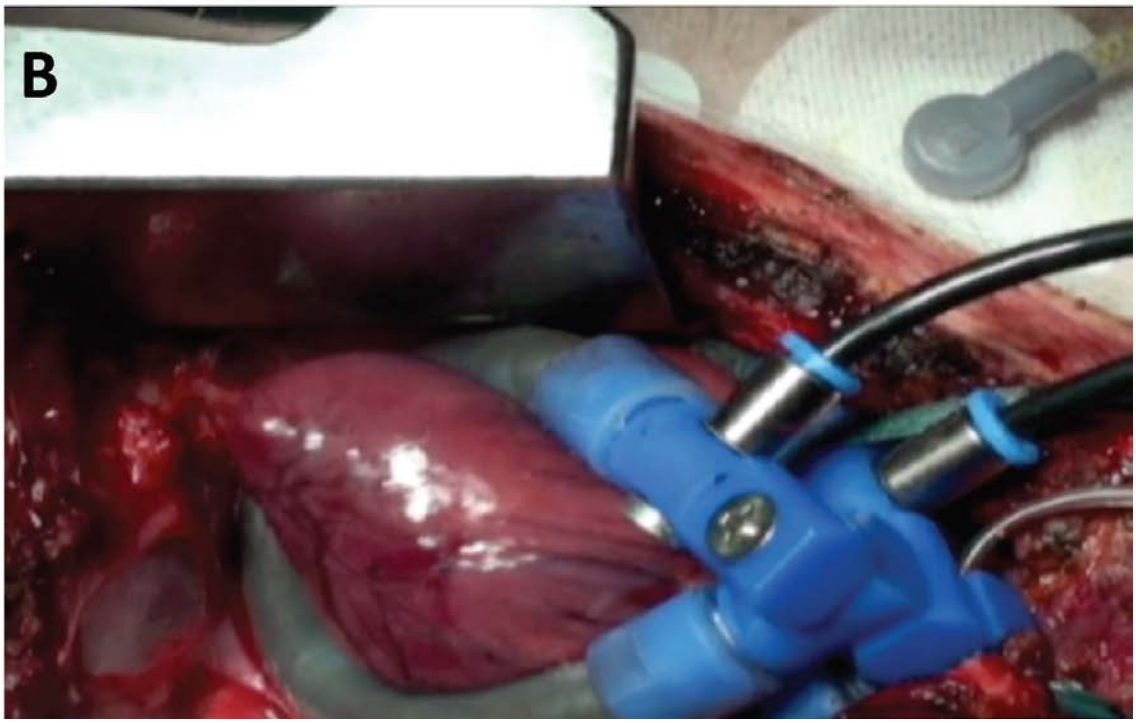
B

Fig. 3

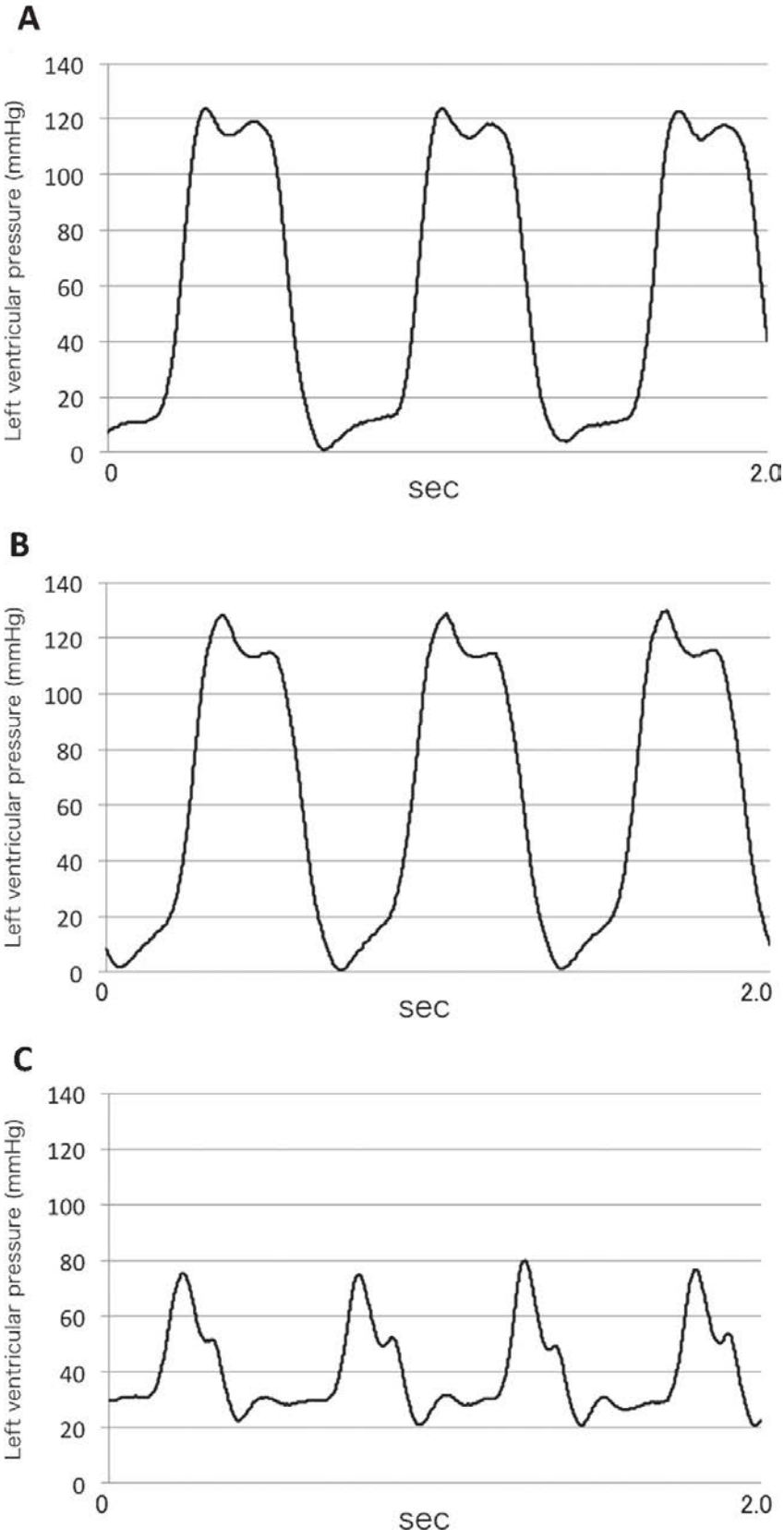
A
Left ventricular pressure (mmHg)
140
120
100
80
60
40
20
0
0
sec
2.0
B
Left ventricular pressure (mmHg)
140
120
100
80
60
40
20
0
0
sec
2.0
C
Left ventricular pressure (mmHg)
140
120
100
80
60
40
20
0
0
sec
2.0

Fig. 4